Phase portraits of the two-body problem with Manev potential

2001 J. Phys. A: Math. Gen. 34 1919

(http://iopscience.iop.org/0305-4470/34/9/309)

INSTITUTE OF PHYSICS PUBLISHING JOURNAL OF PHYSICS A: MATHEMATICAL AND GENERAL

J. Phys. A: Math. Gen. **34** (2001) 1919–1934 www.iop.org/Journals/ja PII: S0305-4470(01)18110-2

Phase portraits of the two-body problem with Manev potential

Jaume Llibre[1], Antonio E Teruel[1], Claudia Valls[2] and Alex de la Fuente[1]

[1] Departament de Matemàtiques, Universitat Autònoma de Barcelona, 08193 – Bellaterra, Barcelona, Spain
[2] Departament de Matemàtica Aplicada i Anàlisi, Universitat de Barcelona, Gran Via de les Cors Catalanes, 585; 08007 Barcelona, Spain

E-mail: jllibre@mat.uab.es, teruel@mat.uab.es and claudia@maia.ub.es

Received 13 October 2000

Abstract

The Manev systems are two-body problems defined by a potential of the form $a/r + b/r^2$, where r is the distance between the two particles, and a and b are arbitrary constants. The Hamiltonian $H = (p_r^2 + p_\theta^2/r^2)/2 + a/r + b/r^2$ and the angular momentum $p_\theta = r^2\dot{\theta}$ associated with Manev systems are two first integrals, which are independent and in involution. Let I_h (respectively I_c) be the set of points of the phase space on which H (respectively p_θ) takes the value h (respectively c). Since H and p_θ are first integrals, the sets I_h, I_c and $I_{hc} = I_h \cap I_c$ are invariant under the flow of the Manev systems. We characterize the global flow of these systems when a and b vary. Thus we describe the foliation of the phase space by the invariant sets I_h and the foliation of I_h by the invariant sets I_{hc}.

PACS numbers: 0425N, 0230H, 0240, 0240M

(Some figures in this article are in colour only in the electronic version; see `www.iop.org`)

1. Introduction

In this paper we describe the global phase portraits of the Manev systems (Maneff in German and French spelling); i.e. a two-body problem defined by the potential of the form $a/r + b/r^2$, where r is the distance between the two particles and a, b are arbitrary constants.

The study of the motion of these two-body problems has a long history. As early as in Newton's work, discrepancies between the observed and theoretical motions of pericentres raised the question concerning the accuracy of the Newtonian inverse square law of gravitation, and motivated the consideration of alternative gravitational models and corrections to reconcile these differences and obtain a satisfactory degree of agreement between the observational evidence and theoretical predictions on the motion of celestial bodies in the solar system; mainly the Moon, but also the planets.

0305-4470/01/091919+16$30.00

Newton was the first to consider the Manev systems with a and b positive. The reason behind Newton's frustration with the inverse square force law was its inability to explain the Moon's perigee motion. A result published in *Principia* (book I, section IX, proposition XLIV, theorem XIV, corollary 2) showed that in this model the motion cannot be an ellipse, but a precessional ellipse; i.e. one that rotates in its own plane of motion. Most of Newton's research on the Manev systems remained unpublished during his life-time. The 1888 catalogue of the *Portsmouth Collection* of unpublished manuscripts that are stored today in the library of Cambridge University shows Newton's interest in this model.

The Manev potential was reconsidered by Clairaut who felt the same frustration when trying to explain the motion of the Moon. Later, however, Clairaut found an argument within the framework of the classical Newtonian model and abandoned the Manev model.

General relativity provided a good theory for gravitation and it was able to answer many important questions in physics and astronomy. Unfortunately, up to now the attempts to formulate a meaningful relativistic n-body problem have failed to provide valuable results. Therefore, as early as the 1920s, there existed the necessity to find a model that could respond to the theoretical needs of celestial mechanics.

It was not easy to find a suitable model that maintains the advantages of the Newtonian one and also makes the necessary corrections such that orbits coming close to collisions match theory with observation. The many pre- and post-relativistic attempts to obtain such models have usually answered certain questions (such as those related to the perihelion advances of the inner planets) but failed to explain other phenomena (such as the Moon's motion). One exception is the potential obtained by Manev [13–16] in the 1920s. More precisely, assigning the mass M to the particle fixed at the origin, the unit of mass to the free particle and denoting $\mu = GM$, $\beta = a/\mu - 1$, $\gamma = 2b\mu$, where G is the constant of gravitation, the Manev potential corresponds to the values $\beta = 0$, $\gamma = 3\mu/c^2$, where c is the speed of light. This model allowed a good theoretical justification of the perihelion advance of mercury and of the other inner planets as well as a description of the Moon's motion. This potential was used by Einstein himself as an approximation of relativity in order to compute the correct perihelion advance of mercury.

The Manev potential fell into oblivion for a half century, then Hagihara [9] pointed out that it provides the same good theoretical approximations as relativity (at least at the solar system level). Manev systems were recently reconsidered in a series of studies having as their starting point Diacu's research [7]. Mioc and Stoica [19, 20] obtained the general solution for its regularized equations, while Diacu *et al* [8] found the analytic solution and the local flow near collisions showing that a black hole effect is present in this model. The isosceles three-body case was studied by Diacu [7].

The two-body problem for the Manev potential with $a, b > 0$ was also tackled. Thus, Lacomba *et al* [11] studied it in Hamiltonian formalism for negative energy; Delgado *et al* [6] provided its analytic, geometric and physical description; Craig *et al* [5] studied it for the anisotropic case. Diacu [7] pointed out the role of this potential among all quasihomogeneous potentials within the framework of the three-body problem. For arbitrary values of a and b the analytic solution has been obtained by Mioc and Stoica [21]; see also the study using canonical variables by Aparicio and Floría [2].

For special values of a and b, various physical and astronomical problems can be modelled, see [6] or [21]. The motion in certain post-Newtonian fields, nonrelativistic (including Manev's one) or relativistic (such as Fock's one [17]) are in such a situation. The motion around an oblate planet [22], the photogravitational field [18, 23] generated by a luminous source, or the two-body problem with an equivalent gravitational parameter [24] also correspond to this model. Connections with atomic physics [25], or astrophysics [7] are also possible.

In this paper we study the global phase portrait of the Manev potential

$$V(r) = \frac{a}{r} + \frac{b}{r^2}$$

with $a, b \in \boldsymbol{R}$, using its formulation as an integrable Hamiltonian system with two degrees of freedom. More precisely, in polar coordinates (r, θ) for the position and (p_r, p_θ) for the momenta, the Hamiltonian which governs the Manev systems is

$$H = \frac{1}{2}\left(p_r^2 + \frac{p_\theta^2}{r^2}\right) + \frac{a}{r} + \frac{b}{r^2}. \tag{1}$$

Its Hamiltonian system is

$$\dot{r} = \frac{\partial H}{\partial p_r} \qquad \dot{\theta} = \frac{\partial H}{\partial p_\theta} \qquad \dot{p_r} = -\frac{\partial H}{\partial r} \qquad \dot{p_\theta} = -\frac{\partial H}{\partial \theta} = 0. \tag{2}$$

Then, the Hamiltonian H and angular momentum p_θ are two first integrals, independent and in involution. Hence, the Hamiltonian system (2) is integrable.

If we denote by $\boldsymbol{R}^+$ the open interval $(0, \infty)$, then the Manev system *phase space* is $E = \boldsymbol{R}^+ \times \boldsymbol{S}^1 \times \boldsymbol{R}^2$ where $r \in \boldsymbol{R}^+$, $\theta \in \boldsymbol{S}^1$ and $(p_r, p_\theta) \in \boldsymbol{R}^2$. Since H and p_θ are first integrals, the sets

$$I_h = \{(r, \theta, p_r, p_\theta) \in E : H(r, \theta, p_r, p_\theta) = h\}$$
$$I_c = \{(r, \theta, p_r, p_\theta) \in E : p_\theta = c\}$$
$$I_{hc} = I_h \cap I_c$$

are invariant by the Hamiltonian flow of (2).

The main results of this paper are the descriptions of the foliations of

(i) the phase space E by the invariant sets I_h,
(ii) I_h by the invariant sets I_{hc}, and
(iii) I_{hc} by the flow of the Hamiltonian system.

These foliations provide a good description of the phase portraits of the Hamiltonian flows defined by (2) when a and b vary.

The paper is organized as follows. In section 2 we recall what the Liouville–Arnold theory states about integrable Hamiltonian systems applied to Manev systems, and what it does not say. In section 3 we describe the sets of critical points and critical values for the map $H : E \to \boldsymbol{R}$. The Hill region R_h is the region of the position space where the motion of all orbits having energy h takes place. In section 4 we classify all Hill regions for the Manev systems according to the different values of a and b. In section 5 we study the topology of the sets I_h when a and b change. Finally, in section 6 we describe the topology of the sets I_{hc} and how these sets foliate I_h.

2. Integrable Hamiltonian systems

In this section we apply the Liouville–Arnold theorem to the integrable Hamiltonian systems (2) defined by the Manev systems. We recall that a flow defined on a subspace of the phase space is called *complete* if its solutions are defined for all time.

Liouville–Arnold theorem (Arnold 1963). *The Hamiltonian system (2) with two degrees of freedom defined on the phase space E has the Hamiltonian H and angular momentum p_θ as two independent first integrals in involution. If $I_{hc} \neq \emptyset$ and (h, c) is a regular value of the map (H, p_θ), then the following statements hold*:

(a) *I_{hc} is a two-dimensional submanifold of E invariant under the flow of (2).*
(b) *If the flow on a connected component I_{hc}^* of I_{hc} is complete, then I_{hc}^* is diffeomorphic either to the torus $\boldsymbol{S}^1 \times \boldsymbol{S}^1$, or to the cylinder $\boldsymbol{S}^1 \times \boldsymbol{R}$. We note that if I_{hc}^* is compact (i.e. $I_{hc}^* \approx \boldsymbol{S}^1 \times \boldsymbol{S}^1$), then the flow on it is always complete.*
(c) *Under the hypothesis (b) the flow on I_{hc}^* is conjugated to a linear flow either on $\boldsymbol{S}^1 \times \boldsymbol{S}^1$, or on $\boldsymbol{S}^1 \times \boldsymbol{R}$.*

For more details about Hamiltonian systems and the proof of the previous theorem see Abraham and Marsden [1] and Arnold [3,4]. We remark that in general, under the assumptions of statement (b), I_{hc}^* can also be diffeomorphic to the plane $\boldsymbol{R}^2$, but this is not the case for the Manev systems, because they are symmetric with respect to the variable θ, and consequently the manifolds I_{hc}^* must have a factor $\boldsymbol{S}^1$.

The Liouville–Arnold theorem shows that, for integrable Hamiltonian systems, the invariant sets associated with the intersections of all independent first integrals in involution are generically submanifolds of the phase space. Moreover, if the flow on such submanifolds is complete, then these submanifolds are diffeomorphic to the union of generalized cylinders and the flow on them is conjugated to a linear flow.

What is not stated by the Liouville–Arnold theorem for our Manev systems is:

(i) What is the topology of the invariant sets I_{hc} when (h, c) is not a regular value of the map (H, p_θ), and how is the flow on these invariant sets?
(ii) How the invariant sets I_{hc} foliate the energy levels I_h?
(iii) How the energy levels I_h foliate the phase space E?

In this paper we solve all these questions for the Manev systems. For a generic study of the invariant sets I_{hc} for Hamiltonian systems of two degrees of freedom having a central potential see Llibre and Nunes [12].

3. Critical values of H

A point $(r, \theta, p_r, p_\theta) \in E$ is *critical* for the map $H : E \to \boldsymbol{R}$ if it is a solution of the system

$$\frac{\partial H}{\partial r} = 0 \qquad \frac{\partial H}{\partial \theta} = 0 \qquad \frac{\partial H}{\partial p_r} = 0 \qquad \frac{\partial H}{\partial p_\theta} = 0. \tag{3}$$

The value $h \in \boldsymbol{R}$ is *critical* for the map $H : E \to \boldsymbol{R}$ if there is some critical point belonging to $H^{-1}(h) = I_h$. If $h \in \boldsymbol{R}$ is not critical, then h is a *regular* value. It is well known that if h is a regular value of the map $H : E \to \boldsymbol{R}$, then I_h is a three-dimensional manifold, see for instance [10].

Since the $r > 0$ system (3) reduces to

$$ar + 2b = 0 \qquad p_r = p_\theta = 0$$

then the set of critical points of H is

$$\mathcal{C} = \{(r, \theta, 0, 0) \in E : ar + 2b = 0 \text{ and } \theta \in \boldsymbol{S}^1\}.$$

Therefore, the set of critical points $\mathcal{C}$ is equal to

$$\begin{array}{ll} \emptyset & \text{if} \quad ab \geqslant 0 \quad \text{and} \quad a^2 + b^2 \neq 0 \\ \{(-2b/a, \theta, 0, 0) \in E : \theta \in \boldsymbol{S}^1\} & \text{if} \quad ab < 0 \end{array}$$

and

$$\{(r, \theta, 0, 0) \in E : (r, \theta) \in \boldsymbol{R}^+ \times \boldsymbol{S}^1\} \qquad \text{if} \quad a^2 + b^2 = 0.$$

Hence, the critical values are $-a^2/(4b)$ if $ab < 0$, and 0 if $a^2 + b^2 = 0$.

4. Hill regions

Let $\pi : E \to \boldsymbol{R}^+ \times \boldsymbol{S}^1$ be the natural projection from the phase space E to the *configuration space* $\boldsymbol{R}^+ \times \boldsymbol{S}^1$. Then for each $h \in \boldsymbol{R}$ the *Hill region* R_h of I_h is defined by $R_h = \pi(I_h)$. Therefore

$$R_h = \left\{(r, \theta) \in \boldsymbol{R}^+ \times \boldsymbol{S}^1 : \frac{a}{r} + \frac{b}{r^2} \leqslant h\right\}$$
$$\approx \{r \in \boldsymbol{R}^+ : hr^2 - ar - b \geqslant 0\} \times \boldsymbol{S}^1 \tag{4}$$

where as usual $\approx$ means diffeomorphic to. Note that the Hill region R_h is the region of the configuration space or position space where the motion of all orbits having energy h takes place.

If $a < 0$ and $b > 0$, then R_h is diffeomorphic to

$$\begin{array}{ll}
\emptyset & \text{if } h < -a^2/(4b) \\
\{a/(2h)\} \times \boldsymbol{S}^1 & \text{if } h = -a^2/(4b) \\
\left[\left(a + \sqrt{a^2 + 4bh}\right)\Big/ (2h),\ \left(a - \sqrt{a^2 + 4bh}\right)\Big/ (2h)\right] \times \boldsymbol{S}^1 & \text{if } -a^2/(4b) < h < 0 \\
[-b/a, \infty) \times \boldsymbol{S}^1 & \text{if } h = 0 \\
\left[\left(a + \sqrt{a^2 + 4bh}\right)\Big/ (2h), \infty\right) \times \boldsymbol{S}^1 & \text{if } h > 0.
\end{array}$$

If $a < 0$ and $b = 0$, then R_h is diffeomorphic to

$$\begin{array}{ll}
(0, a/h] \times \boldsymbol{S}^1 & \text{if } \ h < 0 \\
\boldsymbol{R}^+ \times \boldsymbol{S}^1 & \text{if } \ h \geqslant 0.
\end{array}$$

If $a < 0$ and $b < 0$, then R_h is diffeomorphic to

$$\begin{array}{ll}
\left(0, \left(a - \sqrt{a^2 + 4bh}\right)\Big/ (2h)\right] \times \boldsymbol{S}^1 & \text{if } \ h < 0 \\
\boldsymbol{R}^+ \times \boldsymbol{S}^1 & \text{if } \ h \geqslant 0.
\end{array}$$

If $a = 0$ and $b < 0$, then R_h is diffeomorphic to

$$\begin{array}{ll}
\left(0, \sqrt{b/h}\right] \times \boldsymbol{S}^1 & \text{if } \ h < 0 \\
\boldsymbol{R}^+ \times \boldsymbol{S}^1 & \text{if } \ h \geqslant 0.
\end{array}$$

If $a = 0$ and $b = 0$, then R_h is diffeomorphic to

$$\begin{array}{ll}
\emptyset & \text{if } \ h < 0 \\
\boldsymbol{R}^+ \times \boldsymbol{S}^1 & \text{if } \ h \geqslant 0.
\end{array}$$

If $a = 0$ and $b > 0$, then R_h is diffeomorphic to

$$\begin{array}{ll}
\emptyset & \text{if } \ h \leqslant 0 \\
\left[\sqrt{b/h}, \infty\right) \times \boldsymbol{S}^1 & \text{if } \ h > 0.
\end{array}$$

If $a > 0$ and $b > 0$, then R_h is diffeomorphic to

$$\begin{array}{ll}
\emptyset & \text{if } \ h \leqslant 0 \\
\left[\left(a + \sqrt{a^2 + 4bh}\right)\Big/ (2h), \infty\right) \times \boldsymbol{S}^1 & \text{if } \ h > 0.
\end{array}$$

If $a > 0$ and $b = 0$, then R_h is diffeomorphic to

$$\begin{array}{ll}
\emptyset & \text{if } \ h \leqslant 0 \\
[a/h, \infty) \times \boldsymbol{S}^1 & \text{if } \ h > 0.
\end{array}$$

If $a > 0$ and $b < 0$, then R_h is diffeomorphic to

$$\begin{array}{ll}
\left(0, \left(a - \sqrt{a^2 + 4bh}\right) \Big/ (2h)\right] \times \boldsymbol{S}^1 & \text{if} \quad h < 0 \\
(0, -b/a] \times \boldsymbol{S}^1 & \text{if} \quad h = 0 \\
\left\{\left(0, \left(a - \sqrt{a^2 + 4bh}\right) \Big/ (2h)\right] \cup \left[\left(a + \sqrt{a^2 + 4bh}\right) \Big/ (2h), \infty\right)\right\} \times \boldsymbol{S}^1 & \\
\qquad\qquad \text{if} \quad 0 < h < -a^2/(4b) & \\
\boldsymbol{R}^+ \times \boldsymbol{S}^1 & \text{if} \quad h \geqslant -a^2/(4b).
\end{array}$$

5. Energy levels I_h

We compute the energy levels I_h in two different ways. The first way, described in this section, is more direct. The second way, described in the next section, allows one to additionally deduce the foliation of I_h by the invariant sets I_{hc}.

From the definition of I_h we have that

$$I_h = \bigcup_{(r,\theta) \in R_h} E_{(r,\theta)} \tag{5}$$

where

$$E_{(r,\theta)} = \left\{(r, \theta, p_r, p_\theta) \in E : p_r^2 + \frac{p_\theta^2}{r^2} = \frac{2}{r^2}(hr^2 - ar - b)\right\}.$$

Clearly, for each (r, θ) given the set $E_{(r,\theta)}$ is an ellipse, a point, or the empty set if the point (r, θ) belongs to the interior of R_h, to the boundary of R_h, or does not belong to R_h, respectively. Therefore, from (5), the previous section and a little topology, the topology of I_h easily follows according to the different values of h, a and b.

If $a < 0$ and $b > 0$, then I_h is diffeomorphic to

$$\begin{array}{ll}
\emptyset & \text{if} \quad h < -a^2/(4b) \\
\boldsymbol{S}^1 & \text{if} \quad h = -a^2/(4b) \\
\boldsymbol{S}^3 & \text{if} \quad -a^2/(4b) < h < 0 \\
\boldsymbol{S}^3 \setminus \boldsymbol{S}^1 & \text{if} \quad h \geqslant 0.
\end{array}$$

The third statement follows from the fact that

$$R_h \approx \left[\left(a + \sqrt{a^2 + 4bh}\right) \Big/ (2h), \left(a - \sqrt{a^2 + 4bh}\right) \Big/ (2h)\right] \times \boldsymbol{S}^1$$

and that

$$\pi^{-1}\left(\left[\left(a + \sqrt{a^2 + 4bh}\right) \Big/ (2h), \left(a - \sqrt{a^2 + 4bh}\right) \Big/ (2h)\right] \times \{\theta\}\right) \approx \boldsymbol{S}^2$$

for each fixed $\theta \in \boldsymbol{S}^1$. Then, $I_h \approx \boldsymbol{S}^3$ by using the Hopf fibration of $\boldsymbol{S}^3$.

The fourth statement follows from the third removing a circle. This is due to the fact that in the variable r we have a half-closed interval, closed on the left and open on the right, instead of a closed interval. We remark that $\boldsymbol{S}^3 \setminus \boldsymbol{S}^1$ is diffeomorphic to an open solid torus $\boldsymbol{T}^3$ of $\boldsymbol{R}^3$.

If $a \leqslant 0$, $b \leqslant 0$ and $a^2 + b^2 \neq 0$, then I_h is diffeomorphic to

$$\begin{array}{ll}
\boldsymbol{S}^3 \setminus \boldsymbol{S}^1 & \text{if} \quad h < 0 \\
\boldsymbol{S}^3 \setminus \{\boldsymbol{S}^1 \cup \boldsymbol{S}^1\} & \text{if} \quad h \geqslant 0.
\end{array}$$

In the first statement the two removed copies of $\boldsymbol{S}^1$ are disjoint and correspond to the endpoints of the open interval in the variable r. We note that $\boldsymbol{S}^3 \setminus \{\boldsymbol{S}^1 \cup \boldsymbol{S}^1\}$ is diffeomorphic to $\boldsymbol{R} \times \boldsymbol{S}^1 \times \boldsymbol{S}^1$.

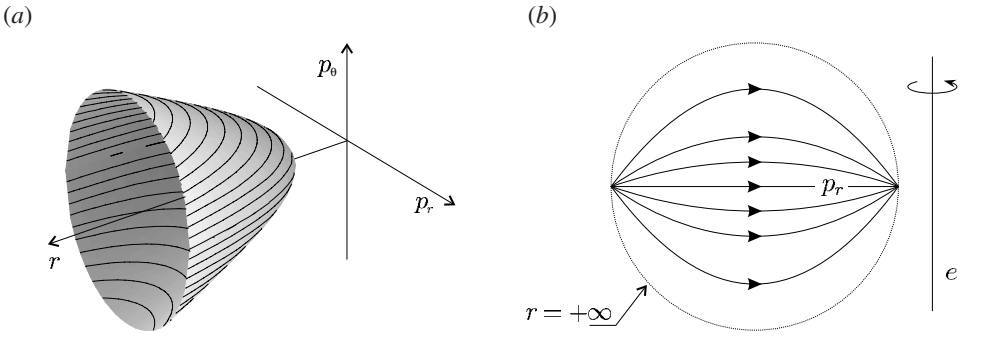

Figure 1. (*a*) The surface $g^{-1}(h)$ for either $a > 0$, $b \geqslant 0$, $h > 0$; $a = 0$, $b > 0$, $h > 0$; or $a < 0$, $b > 0$, $h \geqslant 0$. (*b*) Manifold $I_h/\boldsymbol{S}^1$ for either $a > 0$, $b \geqslant 0$, $h > 0$; $a = 0$, $b > 0$, $h > 0$; or $a < 0$, $b > 0$, $h \geqslant 0$.

If $a \geqslant 0$, $b \geqslant 0$ and $a^2 + b^2 \neq 0$, then I_h is diffeomorphic to

$$\begin{array}{ll} \emptyset & \text{if} \quad h \leqslant 0 \\ \boldsymbol{S}^3 \setminus \boldsymbol{S}^1 & \text{if} \quad h > 0. \end{array}$$

If $a = 0$ and $b = 0$, then I_h is diffeomorphic to

$$\begin{array}{ll} \emptyset & \text{if} \quad h < 0 \\ \boldsymbol{S}^3 \setminus \{\boldsymbol{S}^1 \cup \boldsymbol{S}^1\} & \text{if} \quad h \geqslant 0. \end{array}$$

If $a > 0$ and $b < 0$, then I_h is diffeomorphic to

$$\begin{array}{ll} \boldsymbol{S}^3 \setminus \boldsymbol{S}^1 & \text{if} \quad h \leqslant 0 \\ \{\boldsymbol{S}^3 \setminus \boldsymbol{S}^1\} \cup \{\boldsymbol{S}^3 \setminus \boldsymbol{S}^1\} & \text{if} \quad 0 < h < -a^2/(4b) \\ \boldsymbol{Y} & \text{if} \quad h = -a^2/(4b) \\ \boldsymbol{S}^3 \setminus \{\boldsymbol{S}^1 \cup \boldsymbol{S}^1\} & \text{if} \quad h > -a^2/(4b). \end{array}$$

Here, $\boldsymbol{Y}$ denotes the union of two open solid tori identifying point to point the points of two circles of each torus which cannot be contracted to a single point inside the corresponding torus. This is due to the fact that the $R_h \approx \{(0, a/(2h)] \cup [a/(2h), \infty)\} \times \boldsymbol{S}^1$.

6. Invariant sets I_{hc}

In this section we first compute again the invariant energy levels I_h, but now use the fact that

$$I_h = \{(r, \theta, p_r, p_\theta) \in E : g(r, p_r, p_\theta) = h\} \approx g^{-1}(h) \times \boldsymbol{S}^1 \tag{6}$$

where

$$g(r, p_r, p_\theta) = \frac{1}{2}\left(p_r^2 + \frac{p_\theta^2}{r^2}\right) + \frac{a}{r} + \frac{b}{r^2}.$$

If $h \in \boldsymbol{R}$ is a regular value of the map $g : \boldsymbol{R}^+ \times \boldsymbol{R}^2 \to \boldsymbol{R}$ and $g^{-1}(h) \neq \emptyset$, then $g^{-1}(h)$ is a surface of $\boldsymbol{R}^+ \times \boldsymbol{R}^2$. It is easy to verify that the intersection of $g^{-1}(h)$ with $\{r = r_0 = \text{constant}\}$, is an ellipse, a point, or the empty set according to whether $hr_0^2 - ar_0 - b$ is positive, zero, or negative, respectively. So, by studying the union of the ellipses or points of the form $g^{-1}(h) \cap \{r = r_0\}$ moving $r_0 > 0$, we obtain the sets $g^{-1}(h)$. Therefore, from (6), we calculate in a different way (with respect to the previous section) the topology of the energy levels I_h.

We note that knowing the sets $g^{-1}(h)$, from

$$I_{hc} = I_h \cap \{p_\theta = c\} \approx (g^{-1}(h) \cap \{p_\theta = c\}) \times \boldsymbol{S}^1 \tag{7}$$

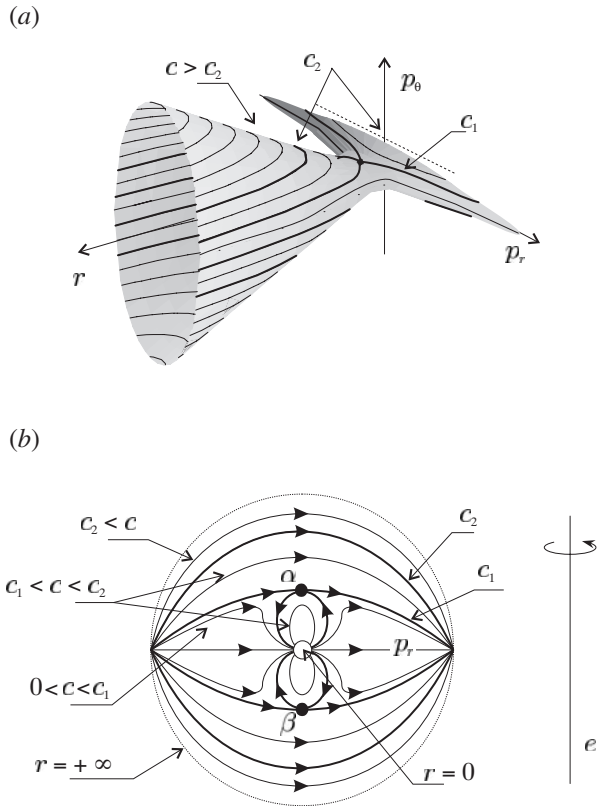

Figure 2. (*a*) The surface $g^{-1}(h)$ for $a > 0$, $b < 0$ and $h > -a^2/(4b)$. (*b*) Manifold $I_h/\boldsymbol{S}^1$ for $a > 0$, $b < 0$ and $h > -a^2/(4b)$.

we can compute the invariant sets I_{hc}. Consequently, we can describe the foliation of I_h by I_{hc} when h varies. In fact we need to study in detail only nine foliations of I_h by I_{hc}, because the study of the remaining cases are topologically equivalent.

Case 1: $a > 0$, $b \geqslant 0$, $h > 0$; $a = 0$, $b > 0$, $h > 0$; *and* $a < 0$, $b > 0$, $h \geqslant 0$. Under these assumptions the surface $g^{-1}(h)$ is the topological plane of figure 1(*a*). The curves $\gamma_{hc} = g^{-1}(h) \cap \{p_\theta = c\}$ for each $c \in \boldsymbol{R}$ are defined for all $r > r(c) > 0$ and homeomorphic to $\boldsymbol{R}$.

The manifold I_h is homeomorphic to $\boldsymbol{S}^3 \setminus \boldsymbol{S}^1$; that is, the solid torus of dimension 3 without a boundary obtained by rotating figure 1(*b*) around the e axis. In this picture we can see how the cylinders I_{hc} foliate the solid torus. We can also see how the flow moves on the cylinders I_{hc}.

Case 2: $a > 0$, $b < 0$ *and* $h > -a^2/(4b)$. Under these assumptions the surface $g^{-1}(h)$ is the topological cylinder of figure 2(*a*). Here, $g^{-1}(h) \cap \{r = r_0\}$ is an ellipse for each $r_0 > 0$. When we consider the curves $\gamma_{hc} = g^{-1}(h) \cap \{p_\theta = c\}$ for each $c \in \boldsymbol{R}$, we need to distinguish four subcases. Thus the curve γ_{hc} has

- two components, each one defined for all $r > 0$ and homeomorphic to $\boldsymbol{R}$, if $0 \leqslant |c| < c_1 = \sqrt{-(a^2 + 4bh)/(2h)}$;

(*a*)

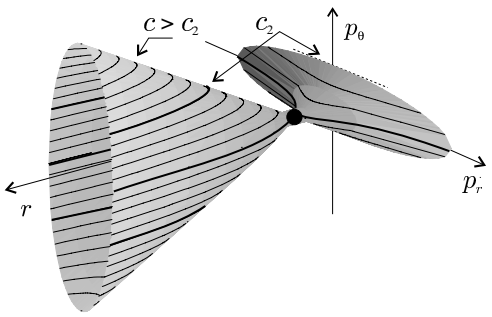

(*b*)

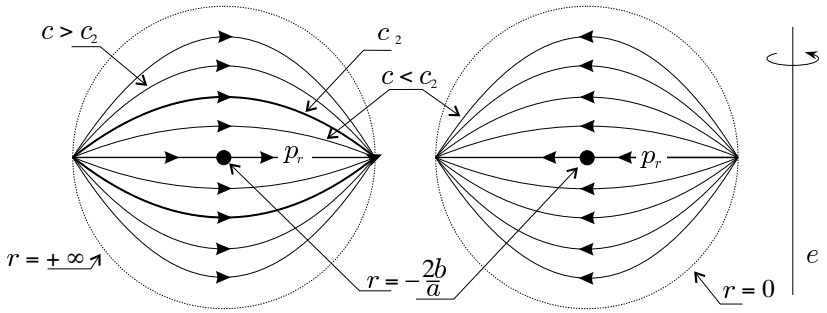

Figure 3. (*a*) The surface $g^{-1}(h)$ for $a > 0$, $b < 0$ and $h = -a^2/(4b)$. (*b*) Manifold $I_h/\boldsymbol{S}^1$ for $a > 0$, $b < 0$ and $h = -a^2/(4b)$.

- only one component topologically homeomorphic to the shape of the letter X, which can be obtained as a limiting case of the previous statement identifying a point of both components, if $|c| = c_1$;
- two components homeomorphic to $\boldsymbol{R}$, one defined in $0 < r \leqslant r_1$ and the other defined in $r_2 \leqslant r < \infty$ with $r_1 < r_2$, if $c_1 < |c| < c_2 = \sqrt{-2b}$ (of course, when $|c|$ tends to c_1 the two curves tend to the unique curve of the previous statement, and r_1 and r_2 tend to the same value); and
- one component homeomorphic to $\boldsymbol{R}$, defined in $0 < r_2 \leqslant r < \infty$, if $c_2 \leqslant |c|$.

The manifold I_h is homeomorphic to $\boldsymbol{S}^3 \setminus \{\boldsymbol{S}^1 \cup \boldsymbol{S}^1\}$. That is, the solid torus of dimension 3 without the boundary and without the central circular axis. This topological space can be obtained by rotating figure 2(*b*) around the *e* axis. In this picture we can see how

- the cylinders I_{hc} for $|c| \geqslant c_2$;
- the two cylinders form I_{hc} for $c_1 < |c| < c_2$;
- the I_{hc} for $c = c_1$ (respectively $c = -c_1$) is formed by the periodic orbit α (respectively β) together with their four invariant cylinders: two of them form the stable manifold of α (respectively β) and the other two the unstable manifold of α (respectively β); and
- the two cylinders form I_{hc} for $0 \leqslant |c| < c_1$;

foliate I_h. We can also see how the flow moves on the I_{hc} surfaces.

Case 3: $a > 0$, $b < 0$ *and* $h = -a^2/(4b)$. Now the surface $g^{-1}(h)$ is the topological cone of figure 3(a). In fact figure 3(a) comes from figure 2(a) collapsing the circle contained in the plane $r = -(2b)/a$ to the point $(r, p_r, p_\theta) = (-(2b)/a, 0, 0)$ when $h > -a^2/(4b)$ tends to $-a^2/(4b)$. When we consider the curves $\gamma_{hc} = g^{-1}(h) \cap \{p_\theta = c\}$ for each $c \in \boldsymbol{R}$, we need to distinguish three subcases. Thus the curve γ_{hc} has

- only one component topologically homeomorphic to the shape of the letter X, if $c = 0$;
- two components homeomorphic to $\boldsymbol{R}$, one defined in $0 < r \leqslant r_1$ and the other defined in $r_2 \leqslant r < \infty$ with $r_1 < r_2$, if $0 < |c| < c_2$ (again, when $|c|$ tends to 0 the two curves tend to the unique curve of the previous statement, and r_1 and r_2 tend to $-(2b)/a$); and
- one component homeomorphic to $\boldsymbol{R}$, defined in $0 < r_2 \leqslant r < \infty$, if $c_2 \leqslant |c|$.

The manifold $I_h \approx \boldsymbol{Y}$ is homeomorphic to two copies of a solid torus without the boundary which have their central circular axis identified. The two copies of the solid torus without the boundary can be obtained by rotating figure 3(b) around the e axis, and I_h is obtained by identifying the central circular axis of both tori. Thus in I_h we can see that

- the central circular axis is a periodic orbit, having two unstable invariant manifolds and two stable invariant manifolds, each of these four manifolds is diffeomorphic to a cylinder, and every solid torus contains one unstable and one stable invariant manifold. The periodic orbit and its four invariant manifolds form the invariant set I_{hc} for $c = 0$;
- two cylinders form I_{hc} for $0 < |c| < c_2$, each contained in a different solid torus;
- one cylinder I_{hc} for $c_2 \leqslant |c|$, these cylinders are contained into the same solid torus.

All these invariant sets I_{hc} foliate I_h, as is shown in figure 3(b). We can also see how the flow moves on the surfaces I_{hc}.

Case 4: $a > 0$, $b < 0$ *and* $0 < h < -a^2/(4b)$. In this case the surface $g^{-1}(h)$ is homeomorphic to two planes, see figure 4(a). Roughly speaking, figure 4(a) comes from figure 3(a) when the cone splits into two topological planes. When we consider the curves $\gamma_{hc} = g^{-1}(h) \cap \{p_\theta = c\}$ for each $c \in \boldsymbol{R}$, we need to distinguish two subcases. Thus the curve γ_{hc} has

- two components homeomorphic to $\boldsymbol{R}$, one defined in $0 < r \leqslant r_1$ and the other defined in $r_2 \leqslant r < \infty$ with $r_1 < r_2$, if $0 \leqslant |c| < c_2$; and
- one component homeomorphic to $\boldsymbol{R}$, defined in $0 < r_2 \leqslant r < \infty$, if $c_2 \leqslant |c|$.

The manifold I_h is homeomorphic to two copies of a solid torus without the boundary. It can be obtained by rotating figure 4(b) around the e axis. In this picture we can see that

- two cylinders I_{hc} for $0 \leqslant |c| < c_2$ (each contained in a different solid torus);
- one cylinder I_{hc} for $c_2 \leqslant |c|$ (these cylinders are contained in the same solid torus);

that foliate I_h. We can also see how the flow moves on the cylinders I_{hc}.

Case 5: $a > 0$, $b < 0$, $h \leqslant 0$*; and* $a = 0$, $b < 0$, $h < 0$. Under these assumptions the surface $g^{-1}(h)$ is the topological plane of figure 5(a). The curves $\gamma_{hc} = g^{-1}(h) \cap \{p_\theta = c\}$ for each $c \in \boldsymbol{R}$ are defined for all r in $0 < r < r(c)$ and are homeomorphic to $\boldsymbol{R}$.

The manifold I_h is homeomorphic to a solid torus without the boundary. It can be obtained by rotating figure 5(b) around the e axis. In this picture we can see one cylinder I_{hc} for every $c \in \boldsymbol{R}$ foliating I_h. We can also see how the flow moves on the cylinders I_{hc}.

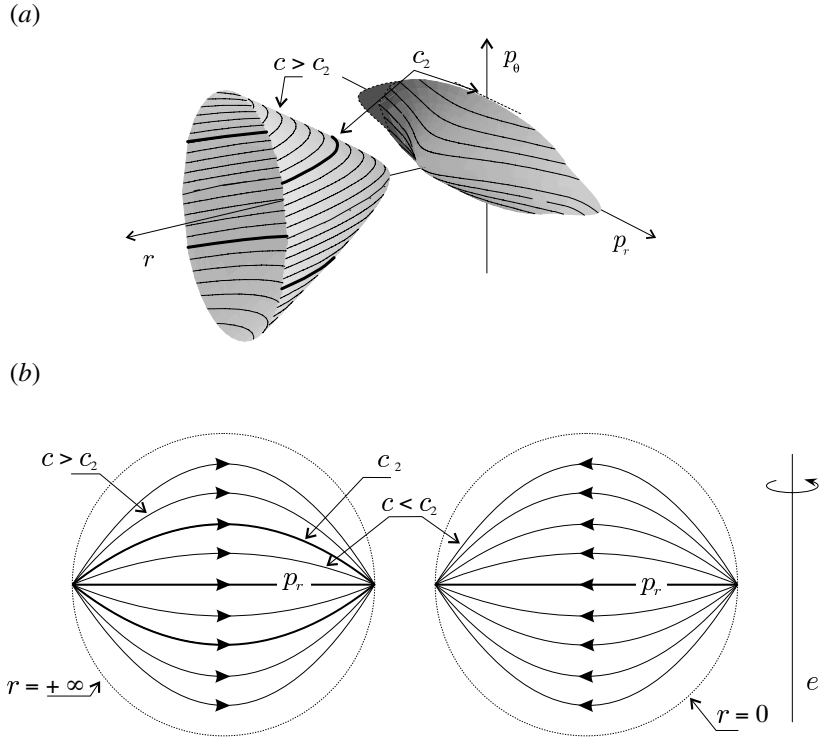

Figure 4. (*a*) The surface $g^{-1}(h)$ for $a > 0$, $b < 0$ and $0 < h < -a^2/(4b)$. (*b*) Manifold $I_h/\boldsymbol{S}^1$ for $a > 0$, $b < 0$ and $0 < h < -a^2/(4b)$.

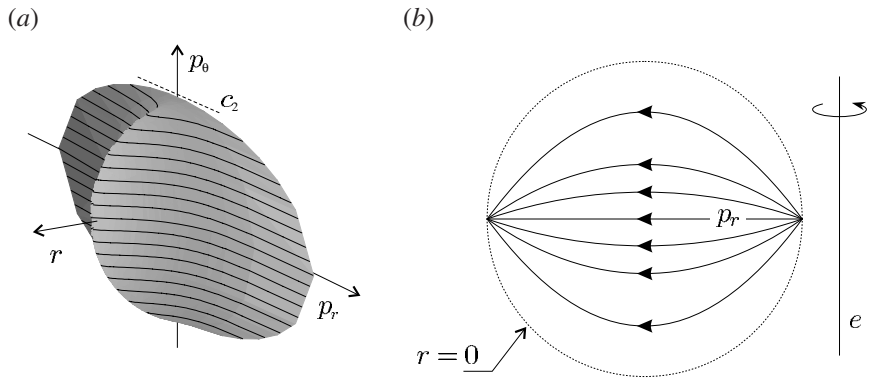

Figure 5. (*a*) The surface $g^{-1}(h)$ for $a > 0, b < 0, h \leqslant 0$; and $a = 0, b < 0, h < 0$. (*b*) Manifold $I_h/\boldsymbol{S}^1$ for $a > 0, b < 0, h \leqslant 0$; and $a = 0, b < 0, h < 0$.

Case 6: $a = 0$, $b = 0$, $h > 0$*; and* $a < 0$, $b \leqslant 0$, $h \geqslant 0$. In this case the surface $g^{-1}(h)$ is homeomorphic to a cylinder $\boldsymbol{S}^1 \times \boldsymbol{R}$, see figure 6(*a*). When we consider the curves $\gamma_{hc} = g^{-1}(h) \cap \{p_\theta = c\}$ for each $c \in \boldsymbol{R}$, we need to distinguish two subcases. Thus the curve γ_{hc} has

- one component homeomorphic to $\boldsymbol{R}$ if $c \neq 0$; and
- two components each homeomorphic to $\boldsymbol{R}$ if $c = 0$.

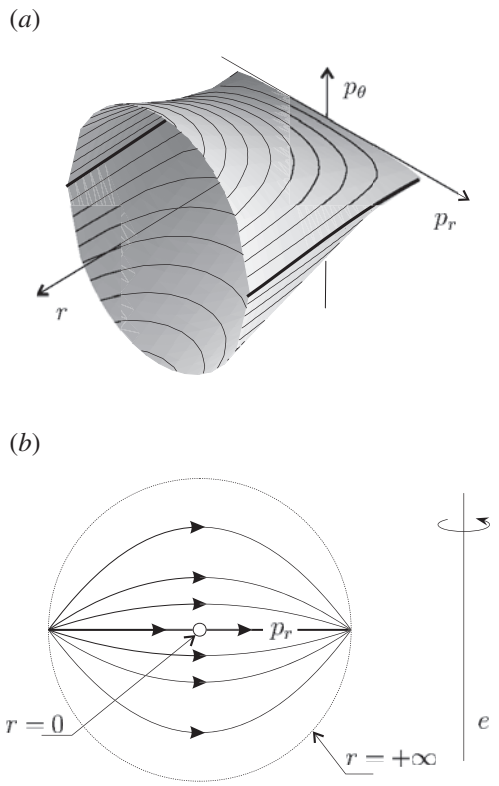

Figure 6. (*a*) The surface $g^{-1}(h)$ for $a = 0, b = 0, h > 0$; and $a < 0, b \leqslant 0, h \geqslant 0$. (*b*) Manifold $I_h/\boldsymbol{S}^1$ for $a = 0, b = 0, h > 0$; and $a < 0, b \leqslant 0, h \geqslant 0$.

The manifold I_h is homeomorphic to a solid torus without the boundary and the central circular axis. It can be obtained by rotating figure 6(*b*) around the e axis. In this picture we can see that

- one cylinder I_{hc} for every $c \in \boldsymbol{R} \setminus \{0\}$; and
- two cylinders I_{hc} for $c = 0$;

foliate I_h. We can also see how the flow moves on the cylinders I_{hc}.

Case 7: $a < 0$, $b > 0$ *and* $-a^2/(4b) < h < 0$. In this case the surface $g^{-1}(h)$ is homeomorphic to a sphere $\boldsymbol{S}^2$, see figure 7(*a*). When we consider the curves $\gamma_{hc} = g^{-1}(h) \cap \{p_\theta = c\}$ for each $c \in \boldsymbol{R}$, we need to distinguish two subcases. Thus the curve γ_{hc} has

- one component homeomorphic to a point if $|c| = c_1$; and
- one component homeomorphic to $\boldsymbol{S}^1$ if $0 \leqslant |c| < c_1$.

The manifold I_h is homeomorphic to $\boldsymbol{S}^3$. In this case $\boldsymbol{S}^3$ is foliated by the I_{hc} as in the Hopf foliation, i.e. I_{hc} is a periodic orbit (topologically a circle) when $|c| = c_1$, and a two-dimensional torus when $|c| < c_1$. This foliation is presented in figure 7(*b*), where we can obtain the sphere $\boldsymbol{S}^3$ identifying the points (of the two surfaces of the cones glued by their bases) which are symmetric with respect to the plane containing the common bases. We can also see how the flow moves on the torus I_{hc} for $|c| < c_1$.

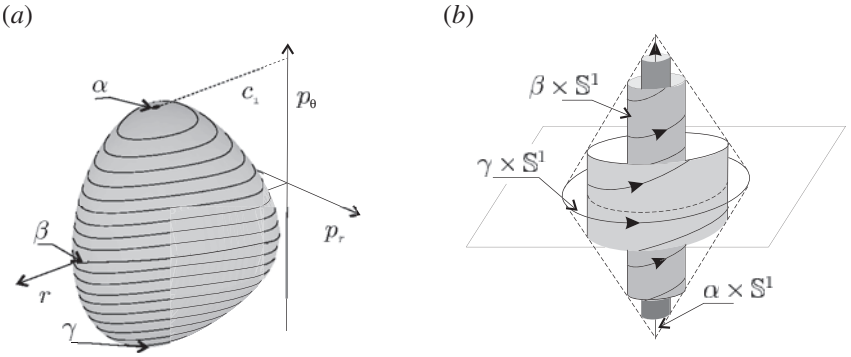

Figure 7. (*a*) The surface $g^{-1}(h)$ for $a < 0, b > 0, -a^2/(4b) < h < 0$. (*b*) Manifold I_h (modulo identifications) for $a < 0, b > 0, -a^2/(4b) < h < 0$.

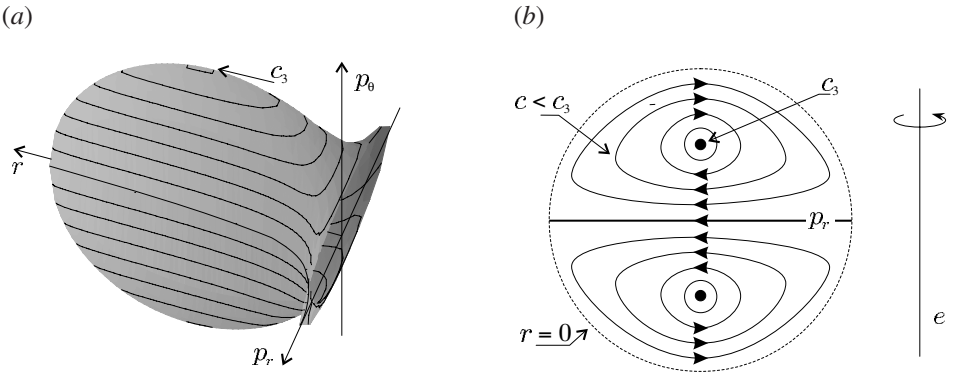

Figure 8. (*a*) The surface $g^{-1}(h)$ for $a < 0, b = 0, h < 0$. (*b*) Manifold $I_h/\boldsymbol{S}^1$ for $a < 0, b = 0, h < 0$.

Case 8: $a < 0, b = 0, h < 0$. Under these assumptions the surface $g^{-1}(h)$ is the topological plane of figure 8(*a*). The curves $\gamma_{hc} = g^{-1}(h) \cap \{p_\theta = c\}$ for each $|c| \leqslant c_3$ are defined for all r in $0 < r < r(c)$ and are homeomorphic to

- one component homeomorphic to a point if $|c| = c_3$;
- one component homeomorphic to $\boldsymbol{S}^1$ if $0 < |c| < c_3$; and
- one component homeomorphic to $\boldsymbol{R}$ if $c = 0$.

The manifold I_h is homeomorphic to a solid torus without the boundary. It can be obtained by rotating figure 8(*b*) around the e axis. In this picture we can see that

- one cylinder I_{hc} for $c = 0$;
- one two-dimensional torus I_{hc} for $0 < |c| < c_3$; and
- one periodic orbit (topologically a circle) I_{hc} for $|c| = c_1$;

foliate I_h. We can also see how the flow moves on the surfaces I_{hc}.

Case 9: $a < 0, b < 0, h < 0$. Under these assumptions the surface $g^{-1}(h)$ is the topological plane of figure 9(*a*). The curves $\gamma_{hc} = g^{-1}(h) \cap \{p_\theta = c\}$ for each $|c| \leqslant c_1$ are defined for all r in $0 < r < r(c)$ and are homeomorphic to

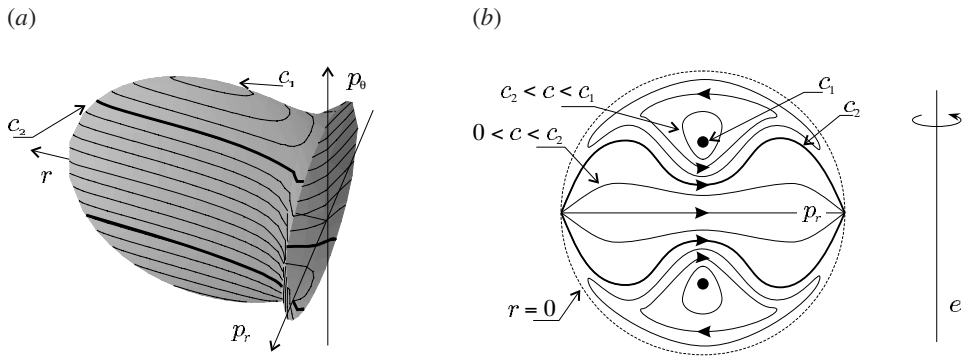

Figure 9. (*a*) The surface $g^{-1}(h)$ for $a < 0, b < 0, h < 0$. (*b*) Manifold $I_h/\boldsymbol{S}^1$ for $a < 0, b < 0$, $h < 0$.

Table 1. The invariant set I_h and its foliation by I_{hc} for $a > 0$.

		I_h	$g^{-1}(h)$	I_{hc}		$I_h/\boldsymbol{S}^1$
$b > 0$	$h > 0$	$\boldsymbol{S}^3 \setminus \boldsymbol{S}^1$	1*a*	$\boldsymbol{S}^1 \times \boldsymbol{R}$	if $c \in \boldsymbol{R}$	1*b*
	$h \leqslant 0$	$\emptyset$		$\emptyset$		
$b = 0$	$h > 0$	$\boldsymbol{S}^3 \setminus \boldsymbol{S}^1$	1*a*	$\boldsymbol{S}^1 \times \boldsymbol{R}$	if $c \in \boldsymbol{R}$	1*b*
	$h \leqslant 0$	$\emptyset$		$\emptyset$		
$b < 0$	$h > -\dfrac{a^2}{4b}$	$\boldsymbol{S}^3 \setminus \{\boldsymbol{S}^1 \cup \boldsymbol{S}^1\}$	2*a*	$\bigcup_2 \boldsymbol{S}^1 \times \boldsymbol{R}$	if $0 \leqslant \lvert c\rvert < c_1$	2*b*
				$\bigcup_2^{\boldsymbol{S}^1} \boldsymbol{S}^1 \times \boldsymbol{R}$	if $\lvert c\rvert = c_1$	
				$\bigcup_2 \boldsymbol{S}^1 \times \boldsymbol{R}$	if $c_1 < \lvert c\rvert < c_2$	
				$\boldsymbol{S}^1 \times \boldsymbol{R}$	if $c_2 \leqslant \lvert c\rvert$	
	$h = -\dfrac{a^2}{4b}$	$\boldsymbol{Y}$	3*a*	$\bigcup_2^{\boldsymbol{S}^1} \boldsymbol{S}^1 \times \boldsymbol{R}$	if $c = 0$	3*b*
				$\bigcup_2 \boldsymbol{S}^1 \times \boldsymbol{R}$	if $0 < \lvert c\rvert < c_2$	
				$\boldsymbol{S}^1 \times \boldsymbol{R}$	if $c_2 \leqslant \lvert c\rvert$	
	$0 < h < -\dfrac{a^2}{4b}$	$\bigcup_2 (\boldsymbol{S}^3 \setminus \boldsymbol{S}^1)$	4*a*	$\bigcup_2 \boldsymbol{S}^1 \times \boldsymbol{R}$	if $0 \leqslant \lvert c\rvert < c_2$	4*b*
				$\boldsymbol{S}^1 \times \boldsymbol{R}$	if $\lvert c\rvert \geqslant c_2$	
	$h \leqslant 0$	$\boldsymbol{S}^3 \setminus \boldsymbol{S}^1$	5*a*	$\boldsymbol{S}^1 \times \boldsymbol{R}$	if $0 \leqslant \lvert c\rvert < c_2$	5*b*

- one component homeomorphic to a point if $|c| = c_1$;
- one component homeomorphic to $\boldsymbol{S}^1$ if $c_2 < |c| < c_1$; and
- one component homeomorphic to $\boldsymbol{R}$ if $0 \leqslant c \leqslant c_2$.

The manifold I_h is homeomorphic to a solid torus without the boundary. It can be obtained by rotating figure 9(*b*) around the e axis. In this picture we can see that

- one cylinder I_{hc} for $0 \leqslant |c| \leqslant c_2$;
- one two-dimensional torus I_{hc} for $c_2 < |c| < c_1$; and
- one periodic orbit (topologically a circle) I_{hc} for $|c| = c_1$;

Table 2. The invariant set I_h and its foliation by I_{hc} for $a = 0$.

		I_h	$g^{-1}(h)$	I_{hc}		$I_h/\boldsymbol{S}^1$
$b > 0$	$h > 0$	$\boldsymbol{S}^3 \setminus \boldsymbol{S}^1$	1a	$\boldsymbol{S}^1 \times \boldsymbol{R}$	if $c \in \boldsymbol{R}$	1b
	$h \leqslant 0$	$\emptyset$		$\emptyset$		
$b = 0$	$h > 0$	$\boldsymbol{S}^3 \setminus \{\boldsymbol{S}^1 \cup \boldsymbol{S}^1\}$	6a	$\bigcup_2 \boldsymbol{S}^1 \times \boldsymbol{R}$	if $c = 0$	6b
				$\boldsymbol{S}^1 \times \boldsymbol{R}$	if $\lvert c\rvert \neq 0$	
	$h = 0$	$\boldsymbol{R} \times \boldsymbol{S}^1$		$\boldsymbol{S}^1 \times \boldsymbol{R}$	if $c = 0$	
	$h < 0$	$\emptyset$		$\emptyset$		
$b < 0$	$h \geqslant 0$	$\emptyset$		$\emptyset$		
	$h < 0$	$\boldsymbol{S}^3 \setminus \boldsymbol{S}^1$	5a	$\boldsymbol{S}^1 \times \boldsymbol{R}$	if $0 \leqslant \lvert c\rvert < c_2$	5b

Table 3. The invariant set I_h and its foliation by I_{hc} for $a < 0$.

		I_h	$g^{-1}(h)$	I_{hc}		$I_h/\boldsymbol{S}^1$
$b > 0$	$h \geqslant 0$	$\boldsymbol{S}^3 \setminus \boldsymbol{S}^1$	1a	$\boldsymbol{S}^1 \times \boldsymbol{R}$	if $c \in \boldsymbol{R}$	1b
	$-\frac{a^2}{4b} < h < 0$	$\boldsymbol{S}^3$	7a	$\boldsymbol{S}^1$	if $\lvert c\rvert = c_1$	
				$\boldsymbol{S}^1 \times \boldsymbol{S}^1$	if $0 \leqslant \lvert c\rvert < c_1$	
	$h = -\frac{a^2}{4b}$	$\boldsymbol{S}^1$		$\boldsymbol{S}^1$	if $c = 0$	
	$h < -\frac{a^2}{4b}$	$\emptyset$		$\emptyset$		
$b = 0$	$h \geqslant 0$	$\boldsymbol{S}^3 \setminus \{\boldsymbol{S}^1 \cup \boldsymbol{S}^1\}$	6a	$\bigcup_2 \boldsymbol{R} \times \boldsymbol{S}^1$	if $c = 0$	6b
				$\boldsymbol{R} \times \boldsymbol{S}^1$	if $\lvert c\rvert \neq 0$	
	$h < 0$	$\boldsymbol{S}^3 \setminus \boldsymbol{S}^1$	8a	$\boldsymbol{S}^1$	if $\lvert c\rvert = c_3$	8b
				$\boldsymbol{S}^1 \times \boldsymbol{S}^1$	if $0 < \lvert c\rvert < c_3$	
				$\boldsymbol{S}^1 \times \boldsymbol{R}$	if $c = 0$	
$b < 0$	$h \geqslant 0$	$\boldsymbol{S}^3 \setminus \{\boldsymbol{S}^1 \cup \boldsymbol{S}^1\}$	6a	$\bigcup_2 \boldsymbol{R} \times \boldsymbol{S}^1$	if $\leqslant \lvert c\rvert \leqslant c_2$	6b
				$\boldsymbol{R} \times \boldsymbol{S}^1$	if $\lvert c\rvert > c_2$	
	$h < 0$	$\boldsymbol{S}^3 \setminus \boldsymbol{S}^1$	9a	$\boldsymbol{S}^1$	if $\lvert c\rvert = c_1$	9b
				$\boldsymbol{S}^1 \times \boldsymbol{S}^1$	if $c_2 < \lvert c\rvert < c_1$	
				$\boldsymbol{R} \times \boldsymbol{S}^1$	if $0 \leqslant \lvert c\rvert \leqslant c_2$	

foliate I_h. We can also see how the flow moves on the surfaces I_{hc}.

In tables 1–3, we summarize the foliation of I_h by I_{hc} for all values of a and b. In these tables we have that $c_1 = \sqrt{-(a^2 + 4bh)/(2h)}$, $c_2 = \sqrt{-2b}$ and $c_3 = \sqrt{-a^2/(2h)}$.

7. Conclusions

The paper provides a description of the global flow of the two–body problem defined by the Manev potential of the form $a/r + b/r^2$, where r is the distance between two particles which are moving in a plane. This motion is of interest in many different kinds of physical and astronomical problems.

The problem here considered is a particular case of an integrable Hamiltonian system with two degrees of freedom. The two first integrals, which are independent and in involution are the Hamiltonian H and the angular momentum p_θ. Then the phase space is foliated by the invariant sets l_{hc}, i.e. the set of points $(r, \theta, p_r, p_\theta)$ of the phase space having $H(r, \theta, p_r, p_\theta) = h$ and $p_\theta = c$. One of the main contributions of this paper is the study and classification of the invariant sets I_{hc}.

Acknowledgments

The first two authors are partially supported by a DGYCIT grant number PB96–1153. The third author is partially supported by a DGYCIT grant number PB94–0215.

References

[1] Abraham R and Marsden J E 1978 *Foundations of Mechanics* (Reading, MA: Benjamin)
[2] Aparicio I and Floría L 1998 Canonical focal method treatment of a Gylden–Maneff problem *Posters of the IV Catalan Days of Applied Mathematics (Tarragona, Spain)* pp 1–16
[3] Arnold V I 1978 *Mathematical Methods of Classical Mechanics* (Berlin: Springer)
[4] Arnold V I, Kozlov V V and Neishtadt A I 1978 *Dynamical Systems III (Encyclopaedia of Mathematical Sciences)* (Berlin: Springer)
[5] Craig S, Diacu F N, Lacomba E A and Perez E 1999 On the anisotropic Manev problem *J. Math. Phys.* **40** 1359–75
[6] Delgado J, Diacu F N, Lacomba E A, Mingarelli A, Mioc V, Perez E and Stoica C 1996 The global flow of the Manev problem *J. Math. Phys.* **37** 2748–61
[7] Diacu F N 1993 The planar isosceles problem fro Maneff's gravitational law *J. Math. Phys.* **34** 5671–90
[8] Diacu F N, Mingarelli A, Mioc V and Stoica C 1995 The Manev two-body problem: quantitative and qualitative theory *Dynamical Systems and Applications (World Sci. Ser. Appl. Anal. vol 4)* (River Edge, NJ: World Science Publishing) pp 213–27
[9] Hagihara Y 1975 *Celestial Mechanics* vol 2, part I (Cambridge, MA: MIT Press)
[10] Hirsch M W 1976 *Differential Topology (Graduate Texts in Math. vol 33)* (New York: Springer)
[11] Lacomba E A, Llibre J and Nunes A 1991 Invariant tori and cylinders for a class of perturbed Hamiltonian systems *The Geometry of Hamiltonian Systems (Berkeley, CA, 1989) (Math. Sci. Res. Inst. Publ. vol 22)* (New York: Springer) pp 373–85
[12] Llibre J and Nunes A 1994 Separatrix surfaces and invariant manifolds of a class of integrable Hamiltonian systems and their perturbations *Mem. Am. Math. Soc.* **513**
[13] Maneff G 1924 La gravitation et le principe de l'égalité de l'action et de la réaction *Comptes Rendus* **178** 2159–61
[14] Maneff G 1925 Die gravitation und das prinzip von wirkung und gegenwirkung *Z. Phys.* **31** 786–802
[15] Maneff G 1930 Le principe de la moindre action et la gravitation *Comptes Rendus* **190** 963–65
[16] Maneff G 1930 La gravitation et l'énergie au zéro *Comptes Rendus* **190** 1374–7
[17] Mioc V 1994 Elliptic-type motion in Fock's gravitational field *Astron. Nachr.* **315** 175–80
[18] Mioc V and Radu E 1992 Orbits in an anisotropic radiation field *Astron. Nachr.* **313** 353–7
[19] Mioc V and Stoica C 1995 Discussion et résolution complète du problème des deux corps dans le champ gravitationnel de Maneff *C. R. Acad. Sci., Paris* **320** 645–8
[20] Mioc V and Stoica C 1995 Discussion et résolution complète du problème des deux corps dans le champ gravitationnel de Maneff, II *C. R. Acad. Sci., Paris* **321** 961–4
[21] Mioc V and Stoica C On the Maneff-type two-body problem *Preprint*
[22] Moulton F R 1970 *An Introduction to Celestial Mechanics* 2nd revised edn (New York: Dover)
[23] Saslaw W C 1978 Motions around a source whose luminosity changes *Astrophys. J.* **226** 240–52
[24] Selaru D, Cucu-Dumitrescu C and Mioc V 1992 On a two-body problem with periodically changing equivalent gravitational parameter *Astron. Nachr.* **313** 257–63
[25] Ureche V 1995 Free-fall collapse of a homogeneous sphere in Maneff's gravitational field *Rom. Astron. J.* **5**